Mon. Not. R. Astron. Soc. **315**, 534–542 (2000)

Statistical studies of pulsar glitches

A. G. Lyne,★ S. L. Shemar and F. Graham Smith
University of Manchester, Jodrell Bank Observatory, Macclesfield, Cheshire SK11 9DL

Accepted 2000 January 27. Received 1999 November 30; in original form 1999 July 5

ABSTRACT

Shemar & Lyne have previously presented observations and an analysis of 32 glitches and their subsequent relaxations observed in a total of 15 pulsars. These data are brought together in this paper with those published by other authors. We show quantitatively how glitch activity decreases linearly with decreasing rate of slow-down. As indicated previously from studies of the Vela pulsar, the analysis suggests that 1.7 per cent of the moment of inertia of a typical neutron star is normally contained in pinned superfluid which releases its excess angular momentum at the time of a glitch. There is a broad range of glitch amplitude and there is a strong indication that pulsars with large magnetic fields suffer many small glitches while others show a smaller number of large glitches. Transient effects following glitches are very marked in young pulsars and decrease linearly with decreasing rate of slow-down, suggesting that the amount of loosely pinned superfluid decreases with age. We suggest that the low braking index of the Vela and Crab pulsars cannot be caused by a decreasing moment of inertia and should be attributed to step increases in the effective magnetic moment of the neutron star at the glitches.

Key words: pulsars: general – pulsars: individual: Vela – pulsars: individual: Crab.

1 INTRODUCTION

Pulsars show timing irregularities of two kinds: timing noise, which is seen as continuous, noise-like fluctuations in rotation rate; and glitches, which are sudden increases in rotation rate, often followed by a period of relaxation towards the unperturbed pre-glitch rotation trend. Studies of glitches have been limited in the past by the small number of detected glitches. This number has doubled during the past few years, partly due to increased monitoring and partly due to the discovery of many young and frequently glitching pulsars in recent surveys (Clifton et al. 1992; Johnston et al. 1992). The events are widely thought to be caused by a sudden transfer of angular momentum from a faster-rotating component of superfluid to the solid crust of the star. The relaxation occurs over a period of time of the order of hours, months or years. Such long relaxation times are compatible only with the very weak viscous properties characteristic of superfluids, and consequently indicate that the interiors consist at least partly of a superfluid (Baym et al. 1969). The characteristics of a glitch event and the post-glitch relaxation towards a steady state provide a kind of rotational seismology to probe neutron star interiors (Pines 1991; Lyne 1992).

Apart from the study of data on the individual glitches themselves, a thorough statistical analysis requires knowledge of the time-spans of data searched during the monitoring programmes in which the glitches were detected. The monitoring time-spans and parameters from the analysis of glitches and subsequent relaxations presented by Shemar & Lyne (1996) have been combined with results published for other glitches to provide a comprehensive data base for statistical studies. The results and interpretations of these studies are presented in this paper. Three main aspects of glitch behaviour have been investigated: the observed sizes of glitches, glitch activity (the extent to which a pulsar suffers from glitches), and the characteristics of post-glitch relaxations. Finally, the possible implications of the new results on the internal processes of neutron stars are discussed.

2 THE GLITCHES

Shemar & Lyne (1996) presented observations and analysis of 32 glitches and the subsequent relaxations which occurred in a total of 15 pulsars out of a total of 289 objects being monitored. Their observations covered well-defined periods up to the end of 1994. Previously published observations of 17 other glitches have been included in our analysis. Some subsequent observations of glitches have been made but these have not been included in the analysis since the sample would otherwise be less well defined. Our data cover 48 glitches in a total of 18 pulsars. Most of these glitches are large glitches, with fractional frequency increases $\Delta\nu_o/\nu_o \sim 10^{-6}$. Smaller events with $\Delta\nu_o/\nu_o \sim 10^{-9}$ have also been reported in a few pulsars. These include PSRs B1907+00 (Gullahorn et al. 1976), B1951+32 (Foster et al. 1994) and B0740−28 (D'Alessandro et al.

★ E-mail: A.Lyne@jb.man.ac.uk

1993). Although some of these are well-defined glitches, others are difficult to distinguish from timing noise. However, Shemar & Lyne (1996) assess that at least 90 per cent of glitches have been detected within the quoted spans for magnitudes in excess of $\Delta\nu_o/\nu_o \sim 5\times10^{-9}$.

Fig. 1 shows the way in which we characterize a glitch. Best-fitting values of rotation rate and its first differential are established from observations before the glitch; all glitch quantities are offsets from these values. The step in rotation rate $\Delta\nu_o$ is followed by a partial relaxation of $Q\Delta\nu_o$, which may be resolved into several components of amplitude $\Delta\nu_n$, each decaying exponentially with time constant τ_n. As seen in the figure, there may also be a persistent step change $\Delta\dot{\nu}_p$ in the first derivative, i.e. a step increase of $-\Delta\dot{\nu}_p$ in the magnitude of the slow-down rate. There may additionally be a continuing change in slow-down rate, approximately linear in time, extending between glitches; this is characterized as a step $\Delta\ddot{\nu}_p$ in the second derivative. These persistent changes are to be distinguished from values of the derivatives immediately after the glitch, which are affected by the transients; for example, an exponential decaying transient gives an initial rate of change $\Delta\ddot{\nu} = -\Delta\dot{\nu}_n/\tau_n$.

The observed characteristics of the glitches are collated in Table 1. Wherever possible, the original data have been used to obtain the best-fitting values of the step changes in rotation and slow-down rates, and the subsequent exponential recovery. The main parameters are shown relative to their pre-glitch values. The steps are given as the instantaneous relative changes $\Delta\nu_o/\nu_o$ and $\Delta\dot{\nu}_o/\dot{\nu}_o$, whilst the post-glitch behaviour is treated as a single-exponential decay in frequency of the form $\Delta\nu_1 e^{-t/\tau_1}$, together with a constant long-term second derivative, $\dot{\nu}_1$. The quoted errors in these parameters are twice the standard deviations from the fits to the data. The occurrence dates are nominal; for some glitches the date is uncertain to some tens of days. The behaviour of the youngest pulsars, the Crab (PSR B0531+21) and Vela (PSR B0833−45), is more complex than most others, and details for these two pulsars, with earlier references, may be found in Chau et al. (1993), Lyne, Pritchard & Smith (1993) and Lyne et al. (1996). In particular, it should be noted that there are substantial short-term transients which have only been observable in the more intensive monitoring conducted more recently, giving rise to the large values of $\Delta\dot{\nu}_o/\dot{\nu}_o$. The transients have time-scales from hours to many tens of days.

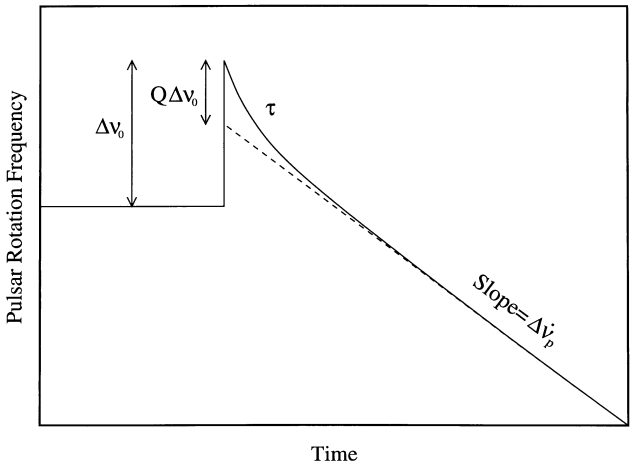

Figure 1. The parameters of an idealized glitch. A fraction Q of the initial step $\Delta\nu_o$ in frequency recovers exponentially on a time-scale τ. The glitch is often accompanied by a permanent step increase in the slow-down rate, $-\Delta\dot{\nu}_p$.

Table 2 summarizes the basic parameters of the pulsars that have glitched, giving the rotational frequency ν, frequency derivative $\dot{\nu}$, characteristic age $\tau_c = P/2\dot{P}$, surface magnetic field strength $B = 3.2\times10^{19}(P\dot{P})^{1/2}$ G and the number of times N_g it has been observed to glitch. The last three columns are the time-span over which the pulsar has been monitored for glitches, the mean fractional increase in rotation rate at the glitches, and the mean observed value of Q, the fraction of the initial change in $\Delta\nu_o$ that is recovered by the exponential.

3 THE DISTRIBUTION OF GLITCH SIZES

The histograms in Fig. 2 show the distribution of glitch size $\Delta\nu_o/\nu_o$ for individual pulsars, together with the aggregate for all glitching pulsars. The histograms extend over a range of 5000:1 in glitch size; they may be incomplete at the lowest level, i.e. 10^{-9}, but there is evidently a significant peak just below the largest glitch at 4.5×10^{-6}. No fewer than eight pulsars contribute to this peak.

The pulsars that usually show the smaller glitches also show smaller intervals between glitches. In Fig. 3 the glitching pulsars are located in a $\nu,\dot{\nu}$ diagram. For each, the width of the diamond is proportional to the apparent rate of glitching, and the height is proportional to the mean size $(\overline{\Delta\nu_o/\nu_o})$. Where a diamond appears as a horizontal line, its height would be less than or equal to the thickness of the line. The apparent glitch rate is simply calculated by dividing the number of glitches that have been detected in the pulsar by the total time-span for which it has been observed. Consequently, the area covered by a diamond is proportional to the glitch activity of the pulsar as defined by McKenna & Lyne (1990). It should be noted that some pulsars have only shown one glitch; we will later group the pulsars to show how glitch activity depends on the rotational parameters in a statistical sense.

This diagram shows that glitches occur most frequently in young pulsars with large slow-down rates. It also shows that pulsars on the left-hand side of the island of pulsars in Fig. 3 generally exhibit smaller glitches than pulsars on the right-hand side. This suggests that the sizes of glitches in a pulsar are dependent upon its rotational frequency. There is also an indication of a possible dependence on magnetic field strength; a similar plot of magnetic field strength B versus characteristic age τ_c is shown in Fig. 4. This plot provides some evidence that in general, for a given characteristic age, pulsars with high B tend to show smaller and more frequent glitches than pulsars with low B. This is particularly evident for PSRs B1338−62, B1737−30, B1758−23 and other young pulsars.

4 INTEGRATED GLITCH ACTIVITY

We now compare the accumulated speeding-up effect of glitches over a long time with the integrated slow-down over the same time. This has already been done for the Vela pulsar (Lyne et al. 1996), where it appears that the integrated amplitude of the glitches is about 2 per cent of the integrated slow-down. The analysis can now be extended statistically to include all pulsars that have been monitored over several years for glitch activity, including those which have not yet glitched. In Table 3, these are divided into 14 groups, each covering a semi-decade of frequency derivative $\dot{\nu}$. In

Table 1. Glitch and relaxation parameters for 18 pulsars.

PSR B	Epoch (MJD)	$\Delta\nu_o/\nu_o$ (10^{-9})	$\Delta\dot{\nu}_o/\dot{\nu}_o$ (10^{-3})	Q (10^{-3})	$\Delta\nu_1/\nu_o$ (10^{-9})	τ_1 (d)	$\ddot{\nu}_1$ ($10^{-24}\,s^{-3}$)	Refs
0355+54	46077(2)	5.5(1)	1.5(4)	–	–	–	8(2)	4
	46497(4)	4368(1)	70(10)	1.12(7)	4.9(3)	165(10)	1.06(4)	4
0525+21	42057(7)	1.3(2)	4.6(9)	500(250)	0.6(3)	145(35)	–	1
0531+21	40493.4	4.0(4)	–	940(10)	–	5(2)	–	10
	42448	44.0(6)	0.22(2)	700(160)	–	15.5(2)	–	10
	46664.42(5)	4.1(1)	2.5(2)	100	4.1(1)	9.3(2)	–	11
	47768.40(2)	85.0(4)	–	–	76.1(3)	18(2)	–	12
	48945.5	4.5(7)	–	–	–	–	–	13
0833−45	40280(4)	2340(10)	10(1)	30(10)	–	–	787	14,15
	41192(8)	2050(30)	15(6)	35(1)	–	–	950	14,15
	42683(3)	1990(10)	10.6(7)	88(8)	–	–	1250	8,14,15
	43693(12)	3060(60)	18(9)	24(5)	–	–	870	8,14,15
	44888.0707(2)	1145(3)	49(4)	183(1)	–	–	1840	14,16
	45192(1)	2050(10)	23(1)	44(3)	–	–	729	14,17
	46257.2284(8)	1601(1)	17(1)	158(1)	–	–	1210	17
	47519.803(1)	1807.1(8)	120(10)	–	–	–	590	18,19
	48457.382(1)	2715(2)	600(60)	–	–	–	1160	20
	49559.057	835(2)	?	–	–	–	–	21
	49591.158	199(2)	120(20)	–	–	–	–	22
1325−43	43590(24)	1.16	–	–	–	–	–	5
1338−62	47989(10)	1505(8)	1(2)	$\lesssim$1	–	–	$\lesssim$50	6
	48453(6)	25(1)	0.15(15)	–	–	–	–	6
	48645(5)	993(2)	1.0(4)	15(5)	15(5)	70(30)	–	6
1535−56	48165(10)	2790.8(2)	−4(1)	$\lesssim$1	–	–	−12(5)	7
1641−45	43390(63)	191(1)	1.6(5)					8
	46453(35)	803.6(1)	0.5(3)					9
	47589(4)	1.61(4)	1.1(1)					9
1706−44	48780(15)	2050(10)	5.3(5)	29(5)	60(10)	190(10)	–	7
1727−33	47990(10)	3080(10)	12(3)	8(1)	24(4)	110(10)	100(2)	4
1736−29	46956(3)	3.09(6)	0.30(6)	–	–	–	–	4
1737−30	47003(25)	420(20)	3(1)	$\lesssim$1	–	–	105(20)	2
	47281(2)	33(5)	2(4)	–	–	–	–	2
	47332(16)	7(5)	−1(12)	–	–	–	–	2
	47458(2)	30(8)	0(4)	–	–	–	65(15)	2
	47670.2(2)	600.9(6)	2.0(4)	$\lesssim$2	–	–	63(10)	2
	48191.9(2)	∼700	–	–	–	–	–	4
	48431(1)	16(1)	0.6(3)	–	–	–	25(2)	4
	49046(2)	9.1(2)	0.17(3)	–	–	–	∼0	4
	49239(1)	169.7(2)	0.74(3)	–	–	–	∼0	4
1758−23	46907(20)	200(30)	−1(3)	$\lesssim$3	–	–	$\lesssim$5	3
	47855(25)	231.2(9)	0.02(4)	$\lesssim$2	–	–	$\lesssim$5	3
	48454(5)	347.68(8)	0.000(1)	$\lesssim$2	–	–	$\lesssim$5	3
1800−21	48245(10)	4075(15)	9.2(4)	15(2)	60(7)	165(5)	128(5)	4
1823−13	46507(30)	$\lesssim$2700	–	–	–	–	199(2)	4
	49014(40)	3060(50)	10(1)	18(1)	54(4)	73(10)	–	4
1830−08	48041(10)	1864.8(3)	1.53(4)	0.8(2)	1.5(3)	205(20)	$\lesssim$5	4
1859+07	46859(3)	30(1)	50(20)	–	–	–	–	4
2224+65	43072(20)	1707(1)	3(5)	–	–	–	0.120(5)	4

Refs: 1. Downs (1982); 2. McKenna & Lyne (1990); 3. Kaspi et al. (1993); 4. Shemar & Lyne (1996); 5. Newton, Manchester & Cooke (1981); 6. Kaspi et al. (1992); 7. Johnston et al. (1995); 8. Manchester et al. (1993); 9. Flanagan (1993); 10. Lohsen (1981); 11. Lyne & Pritchard (1987); 12. Lyne, Smith & Pritchard (1992); 13. Lyne et al. (1993); 14. Cordes, Downs & Krause-Polstorff (1988); 15. Downs (1981); 16. McCulloch et al. (1983); 17. McCulloch et al. (1987); 18. Flanagan (1990); 19. McCulloch et al. (1990); 20. Flanagan (1991); 21. Flanagan (1994a); 22. Flanagan (1994b).

Table 2. Rotational parameters of 18 pulsars that have glitched prior to about MJD 49500.

PSR B	PSR J	ν (Hz)	$\dot{\nu}$ (10^{-15} s^{-2})	τ_c (10^3 yr)	B (10^{12} G)	N_g	Time-span (yr)	$\overline{\Delta\nu_o/\nu_o}$ (10^{-9})	$\bar{Q}$
0355+54	0358+5413	6.4	−180	560	0.8	2	21.7	2200	0.001
0525+21	0528+2200	0.27	−2.9	1480	12.4	1	25.0	1.3	0.5
0531+21	0534+2200	30	−380000	1.2	3.8	5	24.9	28	0.83
0833−45	0835−4510	11	−15700	11	3.4	11	25.8	1760	0.045
1325−43	1328−4357	1.9	−10.7	2800	1.3	1	1.3	1.2	–
1338−62	1341−6220	5.2	−6800	12	7.1	3	3.2	841	0.012
1535−56	1539−5626	4.1	−82.1	800	1.1	1	3.1	2800	<0.001
1641−45	1644−4559	2.2	−97.0	360	3.1	3	14.9	332	<0.0004
1706−44	1709−4428	9.8	−8900	17	3.1	1	4.0	2050	0.029
1727−33	1730−3350	7.2	−4400	26	3.5	1	4.4	3100	0.008
1736−29	1739−2903	3.1	−75.7	650	1.6	1	8.9	3	–
1737−30	1740−3015	1.7	−1270	21	17.0	9	8.5	221	<0.002
1758−23	1801−2306	2.4	−660	60	6.9	3	7.7	260	<0.002
1800−21	1803−2137	7.5	−7600	16	4.3	1	8.1	4100	0.015
1823−13	1826−1334	9.9	−7350	21	2.8	2	8.6	2700	0.018
1830−08	1833−0827	12	−1270	150	0.9	1	7.9	1860	0.0008
1859+07	1901+0716	1.6	−5.8	4500	1.2	1	6.5	30	–
2224+65	2225+6535	1.5	−20.8	1120	2.6	1	12.1	1700	–

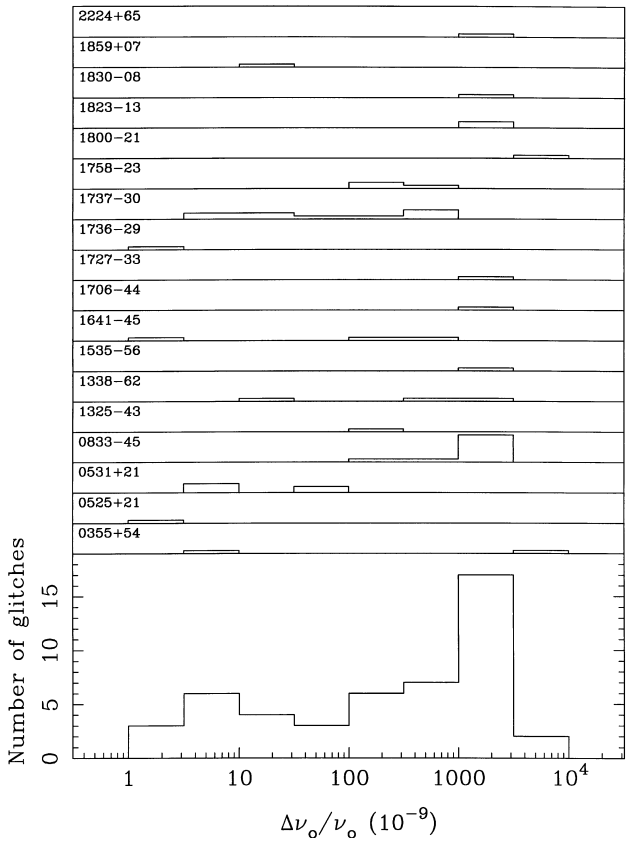

Figure 2. Histograms of glitch size $\Delta\nu_o/\nu_o$ for 48 glitches in 18 individual pulsars. The vertical axis in each case is the number of glitches and ranges from 0 to 10. The lowest diagram shows the total observed distribution of glitch sizes.

each group, $\sum T_i$ is the accumulated years of observation, N_g is the number of glitches observed in the whole group, N_p is the number of pulsars that have glitched, and $\sum\sum\Delta\nu_{ij}$ is the sum of the frequency changes due to glitch j in pulsar i. The mean rate at which rotation rate accumulates through glitches in the whole group is a new parameter, the glitch spin-up rate $\dot{\nu}_{\rm glitch}$, which is defined as

$$\dot{\nu}_{\rm glitch} = \frac{\sum_i \sum_j \Delta\nu_{ij}}{\sum_i T_i}. \quad (1)$$

This is effectively the cumulative effect of glitches upon the slow-down rate $\dot{\nu}$.

The error in each measurement of $\dot{\nu}_{\rm glitch}$ (as shown in brackets in Table 3) is simply taken as $\dot{\nu}_{\rm glitch}/\sqrt{N_g}$. There have been no observations of glitches in pulsars with $-\dot{\nu} < 2.9\times10^{-15}$ s^{-2}, even though the sum of their observed time-spans is quite large and amounts to over 10^3 yr. Upper limits in these groups are obtained by calculating what $\dot{\nu}_{\rm glitch}$ would be if one glitch with $\Delta\nu_o/\nu_o = 10^{-6}$ had occurred within the time-span of observations. The pulsars and time-spans used in this analysis include 279 single pulsars which are being regularly timed at Jodrell Bank, together with observations published by various authors.

Fig. 5 shows the measured values of $\dot{\nu}_{\rm glitch}$ plotted against slow-down rate $-\dot{\nu}$, grouping the pulsars into semi-decade bins of $|\dot{\nu}|$. There is good reason (see Section 8) to consider the youngest pulsars (including the Crab), with $\tau_c < 10^4$ yr, as a separate group, and we consequently look for a relation between activity and $\dot{\nu}$ in pulsars with $\tau_c > 10^4$ yr. Over most of this range, $\dot{\nu}_{\rm glitch}$ is seen to increase approximately linearly with $\dot{\nu}$; the line shown fitted to the upper part of this diagram is given by $\dot{\nu}_{\rm glitch} = -1.7\times10^{-2}\dot{\nu}$. The upper limits in the bins corresponding to the lowest slow-down rates, where several large glitches would have been expected, are barely consistent with this interpretation; as shown, a power law with index 4 would give a better fit. It seems likely that the oldest pulsars, like the millisecond pulsars, are relatively free from glitches. The linear relationship suggests that, apart from the very young and very old pulsars, a fixed fraction 0.017 ± 0.002 of a pulsar's slow-down is on average reversed by glitch activity.

5 POST-GLITCH BEHAVIOUR

The observed post-glitch relaxations in different pulsars can be

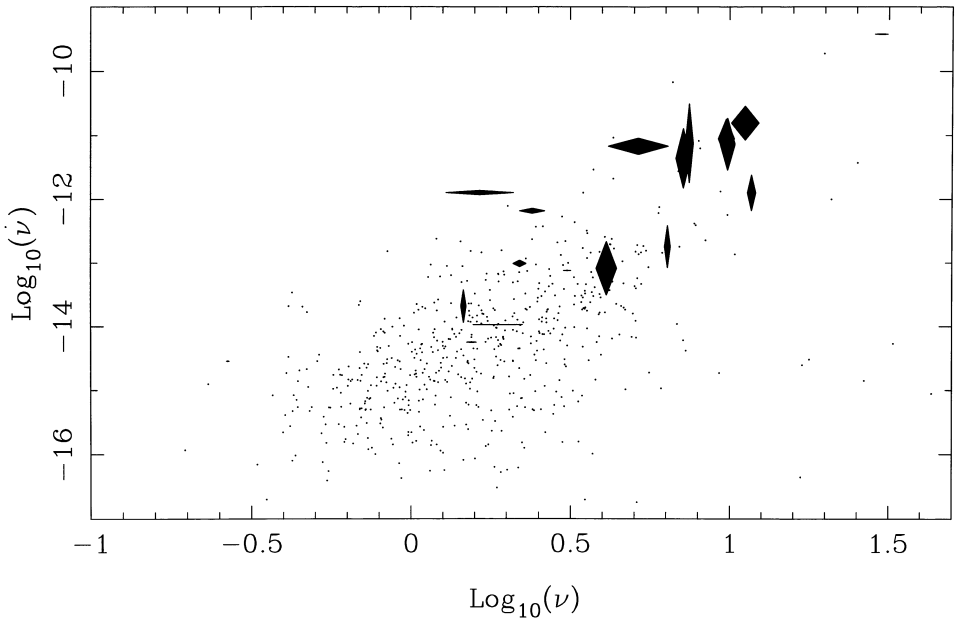

Figure 3. Pulsars that have glitched, shown on a plot of magnitude of frequency derivative $|\dot{\nu}|(s^{-2})$ versus rotational frequency ν (Hz). The height of a diamond is scaled to reflect the mean size $(\overline{\Delta\nu_o}/\nu_o)$ of glitches, while its width reflects the apparent rate of glitches. Where a diamond is replaced by a horizontal line, its height would be less than or equal to the thickness of the line.

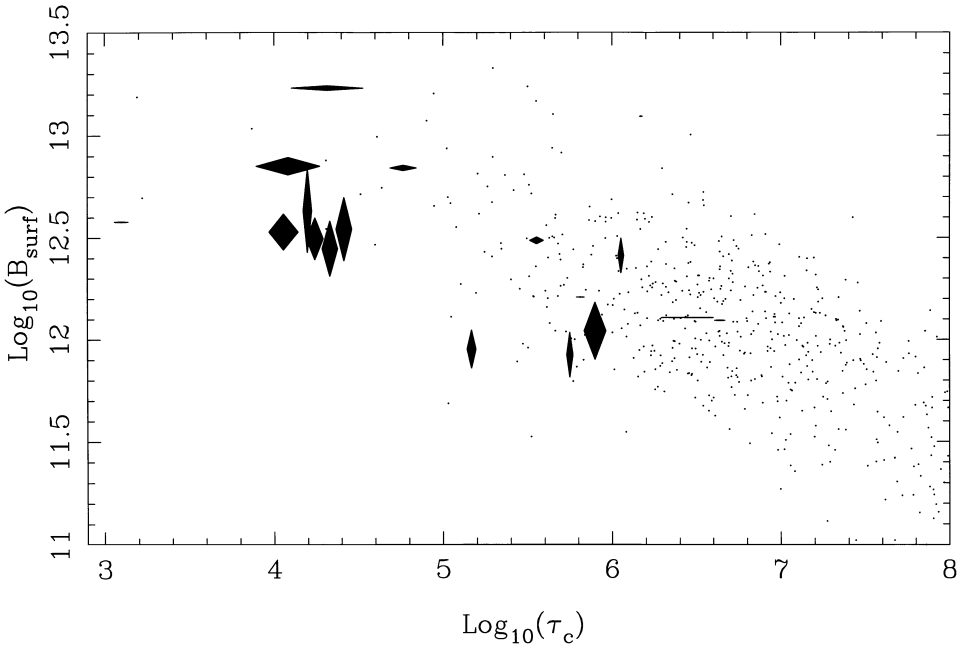

Figure 4. Pulsars that have glitched, shown on a plot of magnetic field strength B (G) versus characteristic age τ_c (yr). The height of a diamond is scaled to reflect the mean size $(\overline{\Delta\nu_o}/\nu_o)$ of glitches, while its width reflects the apparent rate of glitches. Where a diamond is replaced by a horizontal line, its height would be less than or equal to the thickness of the line.

simply described as comprising two distinct decaying components, one short-term and the other long-term. This section discusses the characteristics of these components and any anomalous behaviour that has been observed.

5.1 Short-term relaxation

As in earlier analyses, the short-term exponential decay following the initial step is represented in Table 1 as a fractional recovery $Q = \sum \Delta\nu_n/\Delta\nu_o$. Current theories regard the step and the decay as related to physically separate components. Large values of Q have been observed only for the Crab and Vela pulsars; whether or not these are included, it appears that there may be a functional relation between Q and rotation rate ν or its derivative $\dot{\nu}$. The most significant relation is with $\dot{\nu}$, as shown in Fig. 6. Here we plot a single point for each pulsar; for pulsars that have suffered more than one glitch, we choose the largest, provided that it is well observed, while for the Crab we take the average Q for the

Table 3. The glitch spin-up rate for pulsars in different ranges of $|\dot{\nu}|$.

$\log \lvert\dot{\nu}\rvert$ ($10^{-15}\,s^{-2}$)	$\sum T_i$ (yr)	N_g	N_p	$\sum\sum\Delta\nu_{ij}$ (10^{-6} Hz)	$\dot{\nu}_{glitch}$ ($10^{-15}\,s^{-2}$)
5.50–6.00	25	5	1	3.9	5(2)
5.00–5.50	2	0	0	0	–
4.50–5.00	11	0	0	0	–
4.00–4.50	26	11	1	220	270(100)
3.50–4.00	44	8	5	140	100(35)
3.00–3.50	32	10	2	25	24(8)
2.50–3.00	85	3	1	2.0	0.7(4)
2.00–2.50	192	2	1	28	5(3)
1.50–2.00	316	5	3	14	1.4(6)
1.00–1.50	634	2	2	3.0	0.15(10)
0.50–1.00	562	1	1	0.05	0.003(3)
0.00–0.50	630	1	1	0.0004	0.00002(2)
−0.5–0.00	513	0	0	0	$\lesssim$0.07
−1.0–0.5	205	0	0	0	$\lesssim$0.2

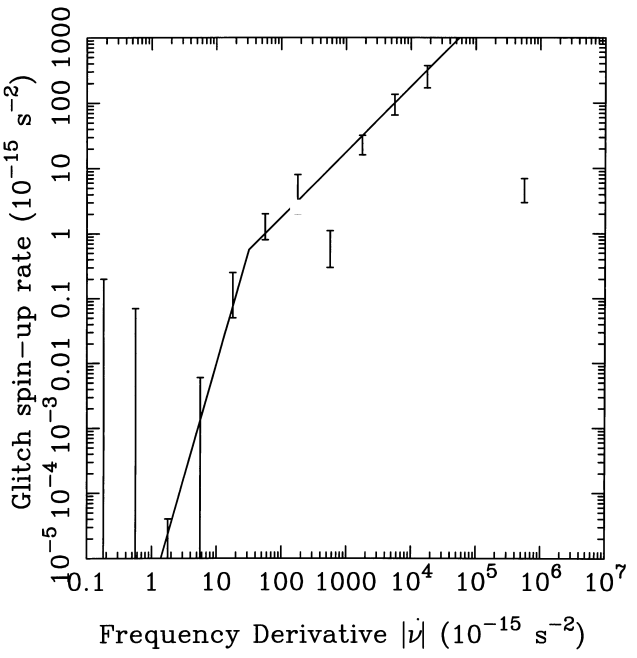

Figure 5. The glitch spin-up rate $\dot{\nu}_{glitch}$ as a function of slow-down rate $|\dot{\nu}|$. The upper portion of the line has a slope of unity, corresponding to $\dot{\nu}_{glitch} = -0.017\dot{\nu}$ (see text).

two largest glitches and for Vela we take the average for the first four. The dashed lines represent upper limits for glitches where no decay has been observed.

Apart from a single point, that for PSR B0525+21, Fig. 6 shows a remarkably close relation between Q and slow-down rate $-\dot{\nu}$. There is no obvious reason to exclude this single discrepant pulsar from the discussion, except that it happens to be the slowest rotator known and is isolated from the other glitching pulsars in Fig. 3.

The time constants τ of these short-term decays range from 18 to 200 d. There is no apparent relation between τ and the main rotational parameters of the pulsars.

5.2 Long-term relaxation

It was first pointed out by Downs (1981) that the behaviour of the Vela pulsar between glitches is well described by a linearly

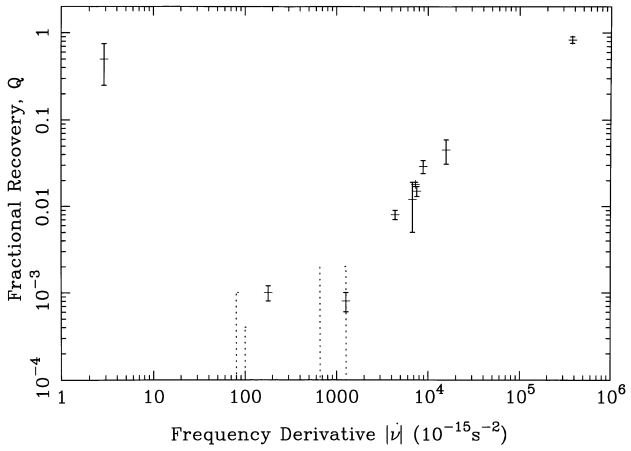

Figure 6. Fractional recovery in rotational frequency Q produced by the exponential decay versus magnitude of frequency derivative $|\dot{\nu}|$ of a pulsar. The dashed lines represent upper limits.

decreasing slow-down rate. This is also observed in several other pulsars, e.g. PSRs B0355+54, B1727−33 and B1800−21 (Shemar & Lyne 1996). In some cases (PSR B1737−30, B2224+65 and the first glitch in PSR B1823−13) there is no observable short-term decay, and such a linear decay describes the whole of the post-glitch behaviour. In addition to these examples, the pre-glitch behaviours of both PSR B1800−21 and PSR B1706−44 also exhibit positive values of $\ddot{\nu}$, which are presumably part of the effects of previously unobserved glitches.

It is of course possible that the apparent linear decays are actually part of exponential decays with large time constants. The post-glitch behaviour of PSR B0355+54 has now been followed for over 3000 d, and there is some indication that an exponential might provide a better fit. However, if the decay is indeed a single exponential, it must have a very large amplitude. From the closeness of the fits to a linear decay, the time constant in this and other examples must be of order 1000 d or more. The amplitude of the exponential would then be greater than $\Delta\dot{\nu}_p$, and greater than the observed step $\Delta\dot{\nu}_o$ (after subtracting the short-term component), since the decay would not be complete before the next glitch.

5.3 The Crab pulsar

The most notable departure from the pattern of behaviour that we analyse in this paper is the post-glitch relaxation of the Crab pulsar. The major difference is that two out of the five glitches observed in this pulsar have left persistent increases in slow-down rate (Lyne et al. 1993). The combined effect of the two largest glitches has produced an apparently permanent increase in slow-down rate of the pulsar of 0.07 per cent over a period of 25 yr. No such effect has been observed in any other pulsar. The Crab pulsar also displayed, after the 1989 glitch, an asymptotic exponential increase in rotation rate, with time constant 250 d; this again is unique. The other two pulsars with similar characteristic ages (PSRs B0540−69, B1509−58) have not yet glitched or been observed for long enough to decide whether they should be considered alongside the Crab or the Vela pulsars, which are very different in their behaviour.

6 SUMMARY OF OBSERVED EFFECTS

The assembly and analysis of glitches in this paper have revealed

the following general characteristics of glitches. For all but the youngest and oldest pulsars:

(i) averaged over a long period of time, a fixed fraction of around 1.7 per cent of the slow-down is reversed by glitch activity;
(ii) the glitch size $\Delta\nu_o/\nu_o$ ranges from 10^{-9}, and possibly smaller, to an upper limit of 5×10^{-6}, more than half lying in the narrow range 3×10^{-7} to 5×10^{-6};
(iii) the ratio Q between the transient and step components is closely related to the general slow-down rate $|\dot{\nu}|$, the largest transients being observed in the youngest pulsars;
(iv) the relaxation after a glitch is usually well fitted by two approximately equal components, designated short- and long-term;
(v) the short-term component is an exponential with time constant of order 100 d which does not depend on age or any other rotational parameter;
(vi) the long-term component is best represented as a monotonic and nearly linear decay in slow-down rate.

These remarks take no account of the very short-term transients observed after glitches in the Crab and Vela pulsars (Lyne et al. 1993; Alpar et al. 1993). It is uncertain whether such effects are present in the older pulsars because they have been monitored less thoroughly.

7 INTERPRETATION IN TERMS OF VORTEX THEORY

These phenomena concern the interaction between the superfluid interior and the solid crust of the neutron star. The pulsar is slowing down due to the external torque of its strong magnetic field. Part of the neutron superfluid can rotate almost independently of the crust, and its rotation slow-down can lag that of the crust. The step increase in the observed crustal rotation rate ν at a glitch is interpreted as being due to a transfer of angular momentum from part of the more rapidly rotating superfluid. The rotation of the superfluid is embodied in quantized vortices, which can pin to the crust. Since the angular momentum of the superfluid is given by the area density of the vortices, the angular velocity of a completely pinned superfluid is constant, and this component can only slow down if the vortices are allowed to move outwards. Pinned vortices are therefore decoupled from the rotation dynamics of the rest of the pulsar. A glitch occurs when a substantial component of the pinned vortices unpins, moves outwards and transfers angular momentum to the crust.

The independently rotating component of the superfluid has been identified by Pines & Alpar (1985) and others as superfluid interpenetrating the inner crust; however Jones (1998) has shown that the pinning energy between the rotational vortices and the crystal lattice is too low for sufficient pinning to occur in this crustal superfluid. Ruderman, Zhu & Chen (1998) propose a model involving the interaction within the core between rotational vortices and magnetic flux tubes. As shown by Muslimov & Tsygan (1985), the expansion of the lattice of vortices within the core due to the overall rotational slow-down is resisted by the much denser array of flux tubes, since the core of a vortex interacts strongly with a flux tube. Ruderman et al. (1998) consider two possibilities: the flux-tube array may move outward with the vortices, or it may be cut through and reconfigured. In either case this will lead to a distortion of the magnetic field at the interface between the core and the crust, so exerting a force on the crust.

Although the crust has a very high conductivity and is very rigid, these internal distortions of the magnetic field may lead to both a slow change in the external magnetic field and a stress within the crust which may exceed the yield strength. The first will affect the long-term rotational dynamics; the second may result in a catastrophic yield, or crust-cracking event, which would be the origin of a glitch. The crust-cracking would initiate a readjustment both of the angular momentum and of the external magnetic field.

In this core–superfluid theory, the behaviour depends on the rate of rotational slow-down and on the rate of magnetic relaxation in the crust. Ruderman et al. (1998) show that these factors can account for many previously unexplained phenomena, notably the distinctive behaviour of young pulsars such as the Crab, and also for the lack of glitches in the slowest pulsars.

In both theories, locating the independently rotating superfluid component within either the crust or the core, there may be part of the superfluid in which there is an equilibrium between pinning and unpinning, such that there may be a continuous 'vortex creep', with a constant offset in rotation rate. The effect of a glitch on such a region is to disturb the equilibrium offset by the step $\Delta\nu_o$ in the rotation rate of the crust; an exponential recovery follows as the equilibrium is re-established. Alpar et al. (1993) develop this model to account for the linear recovery that is also observed in some glitches.

Our analysis of observed glitches bears on these theories in the following way:

(i) *Moment of inertia of the pinned region.* In all except the youngest pulsars (and possibly the oldest), the integrated effect of the step-wise glitches is to reverse 1.7 per cent of the slow-down. This indicates that 1.7 per cent of the moment of inertia of the star is in a region that is normally pinned and releases its excess angular momentum at the time of a glitch.

(ii) *Critical angular velocity.* The glitch may be initiated at a critical angular velocity difference. The concentration of major glitch sizes at $\Delta\nu_o/\nu_o \approx 10^{-6}$, combined with the observation that an approximately constant 1.7 per cent of the angular momentum is contained in the glitching component, indicates that the critical angular velocity difference to initiate a glitch is related to rotation rate, and is approximately $5\times10^{-4}\nu$. This dependence may, of course, be functionally related to some other parameter that changes with age, such as temperature.

(iii) *The creep regions.* The moment of inertia of a continuous creep region is related to that of the stepping pinned region by the ratio Q. For the majority of pulsars Q is of the order 10^{-2}; there appears to be a monotonic decrease with age or $\dot{\nu}$ as seen in Fig. 6. If a region with moment of inertia I_1 is rotating with a steady differential angular velocity that is reduced by the step change $\Delta\nu_o$ in crust angular velocity, the response of the region is an exponential recovery $\Delta\nu_o\exp(-t/\tau_1)$. Angular momentum is transferred to the crust at rate $I_1\tau^{-1}\Delta\nu_o\exp(-t/\tau_1)$, and the crust accelerates as

$$\Delta\dot{\nu}_c = (I_1/I\tau_1)\Delta\nu_o\exp(-t/\tau_1), \quad (2)$$

where I is the moment of inertia of the crust. It follows that the moment of inertia of the creep component is of the order of $10^{-2}I$, possibly increasing in the younger pulsars in proportion to slow-down rate. (It should be noted, however, that the assumption that the step in differential angular velocity can be equated to $\Delta\nu_o$ is not applicable to the Crab pulsar, where the initial step is more complex.)

(iv) *Discrete exponential components.* It is remarkable that a single exponential (or a series of distinct exponentials as in the Vela pulsar) provides a good fit to the post-glitch recovery. Although the regions involved contain only about 2 per cent of the total moment of inertia; they must comprise a wide range of physical conditions, such as temperature and crystal lattice configuration, which would be expected to affect the recovery time constant.

8 THE CRAB AND VELA PULSARS

The two pulsars that have been observed in the greatest detail, namely the Crab and the Vela pulsars, both provide important exceptions to the general pattern of behaviour outlined above. In the Crab pulsar there are no large glitches, but there are large increases in slow-down rate which accumulate at each major glitch. Vortex pinning theory alone would only explain this by accumulations of completely pinned vortices in domains with high angular velocity, which must remain frozen without release at the glitches. In contrast, the core–superfluid theory allows the increase in slow-down rate to be explained as an increase in the dipole magnetic field.

The Vela pulsar has a different anomaly, revealed in its slow-down as measured over a long time-span (Lyne et al. 1996). Theory suggests that it is slowing down according to a simple power law $\dot{\nu} \propto \nu^n$. The 'characteristic age' is then given by $[1/(n-1)]\nu/\dot{\nu}$. It is usually assumed that the index $n = 3$, as expected from the rate of loss of angular momentum through magnetic dipole radiation; all tabulated pulsar characteristic ages $\tau_c = \frac{1}{2}\nu/\dot{\nu}$ are calculated on this assumption. A determination of n from the second differential, using the relation $n = \nu\ddot{\nu}/\dot{\nu}^2$, is rarely possible and may not be reliable; for the Vela pulsar in particular it has hitherto been prevented by the large changes in rotation rate and its derivatives at and between glitches. It now appears that the second differential $\ddot{\nu}$ can be determined from the rotation rate of the Vela pulsar over 25 yr, including the effects of the nine glitches occurring during this time, giving a value for the index $n = 1.4 \pm 0.2$, and an age several times greater than the previously accepted value of 11 000 yr.

In the present context we ask how such a low value of n might be accounted for in the vortex pinning theory, and we propose an explanation in terms of incremental change at the glitches rather than a continuous process that is merely interrupted by the glitches. The step increase in slow-down rate at glitches in the younger Crab pulsar provides a model; we now propose that a similar but larger step is occurring at the Vela glitches. This might be accounted for by a change in either the effective magnetic dipole moment M or the moment of inertia I in the slow-down equation:

$$-\dot{\nu} \propto M^2 I^{-1} \nu^3. \tag{3}$$

If either or both of M and I are changing, then

$$\frac{\mathrm{d}\dot{\nu}}{\dot{\nu}} = 2\frac{\mathrm{d}M}{M} - \frac{\mathrm{d}I}{I} + 3\frac{\mathrm{d}\nu}{\nu}. \tag{4}$$

The low value of $\ddot{\nu}$, which is 1.4 instead of the expected value of 3.0, might then be accounted for either by a change in I amounting to

$$I^{-1}\frac{\mathrm{d}I}{\mathrm{d}t} = 1.6\frac{\dot{\nu}}{\nu} \tag{5}$$

or by a change in M amounting to

$$M^{-1}\frac{\mathrm{d}M}{\mathrm{d}t} = -0.8\frac{\dot{\nu}}{\nu}. \tag{6}$$

Since the conventional characteristic age $\tau_c = -\frac{1}{2}\nu/\dot{\nu}$, the required mean rate of change of I is

$$I^{-1}\frac{\mathrm{d}I}{\mathrm{d}t} = -0.8\tau_c^{-1}, \tag{7}$$

or alternatively the required rate of change of M is

$$M^{-1}\frac{\mathrm{d}M}{\mathrm{d}t} = 0.4\tau_c^{-1}. \tag{8}$$

The first suggests that the effective total moment of inertia is decreasing on a time-scale of 9000 yr; however, if only 2 per cent of total moment of inertia is involved in the pinning and unpinning process, this time-scale becomes very short indeed. The second possibility seems more likely, i.e. that the effective dipole moment is increasing on a time-scale of 18 000 yr. This might be due to a reorganization of the field or to a change in the alignment of the dipole in relation to the rotation axis; both are possible in the core–superfluid theory.

A different explanation for the slow-down law is needed in the Crab pulsar, where the value $n = 2.5$ is determined *between* glitches, not averaged over them as in the Vela pulsar. This case requires a continuously increasing dipole moment, on a time-scale of $4\tau_c$, i.e. 4000 yr. (The average increase of $\dot{\nu}$ due to glitches is 0.001 per cent per year, too small compared with the age of $\sim$1000 yr to affect n). The changes in $\dot{\nu}$ at the Crab glitches may also require an explanation in terms of an increase in dipole moment, so that both continuous and step increases occur in this pulsar. Ruderman et al. (1998) suggest that in this young pulsar there may be a continuous relaxation of the magnetic field within the crust, allowing the external field to increase even between the glitches.

ACKNOWLEDGMENTS

We thank M. Ruderman for helpful comments on an earlier draft of this paper. SLS thanks the Fentham's and Lawrence Atwell's Trusts for financial support during this work.

REFERENCES

Alpar M. A., Chau H. F., Cheng K. S., Pines D., 1993, ApJ, 409, 345
Baym G., Pethick C., Pines D., Ruderman M., 1969, Nat, 224, 872
Chau H. F., McCulloch P. M., Nandkumar R., Pines D., 1993, ApJ, 413, L113
Clifton T. R., Lyne A. G., Jones A. W., McKenna J., Ashworth M., 1992, MNRAS, 254, 177
Cordes J. M., Downs G. S., Krause-Polstorff J., 1988, ApJ, 330, 847
D'Alessandro F., McCulloch P. M., King E. A., Hamilton P. A., McConnell D., 1993, MNRAS, 261, 883
Downs G. S., 1981, ApJ, 249, 687
Downs G. S., 1982, ApJ, 257, L67
Flanagan C. S., 1990, Nat, 345, 416
Flanagan C. S., 1991, IAU Circ. No. 5311
Flanagan C. S., 1993, MNRAS, 260, 643
Flanagan C. S., 1994a, IAU Circ. No. 6038
Flanagan C. S., 1994b, IAU Circ. No. 6064
Foster R. S., Lyne A. G., Shemar S. L., Backer D. C., 1994, AJ, 108, 175
Gullahorn G. E., Payne R. R., Rankin J. M., Richards D. W., 1976, ApJ, 205, L151
Johnston S., Lyne A. G., Manchester R. N., Kniffen D. A., D'Amico N., Lim J., Ashworth M., 1992, MNRAS, 255, 401
Johnston S., Manchester R. N., Lyne A. G., Kaspi V. M., D'Amico N., 1995, A&A, 293, 795
Jones P. B., 1998, MNRAS, 296, 217

Kaspi V. M., Manchester R. N., Johnston S., Lyne A. G., D'Amico N., 1992, ApJ, 399, L155
Kaspi V. M., Lyne A. G., Manchester R. N., Johnston S., D'Amico N., Shemar S. L., 1993, ApJ, 409, L57
Lohsen E. H. G., 1981, A&AS, 44, 1
Lyne A. G., 1992, Phil. Trans. R. Soc. A, 341, 29
Lyne A. G., Pritchard R. S., 1987, MNRAS, 229, 223
Lyne A. G., Smith F. G., Pritchard R. S., 1992, Nat, 359, 706
Lyne A. G., Pritchard R. S., Smith F. G., 1993, MNRAS, 265, 1003
Lyne A. G., Pritchard R. S., Graham-Smith F., Camilo F., 1996, Nat, 381, 497
McCulloch P. M., Hamilton P. A., Royle G. W. R., Manchester R. N., 1983, Nat, 302, 319
McCulloch P. M., Klekociuk A. R., Hamilton P. A., Royle G. W. R., 1987, Aust. J. Phys., 40, 725
McCulloch P. M., Hamilton P. A., McConnell D., King E. A., 1990, Nat, 346, 822
McKenna J., Lyne A. G., 1990, Nat, 343, 349
Manchester R. N., Newton L. M., Hamilton P. A., Goss W. M., 1983, MNRAS, 202, 269
Muslimov A. G., Tsygan A. I., 1985, Ap&SS, 115, 43
Newton L. M., Manchester R. N., Cooke D. J., 1981, MNRAS, 194, 841
Pines D., 1991, in Ventura J., Pines D., eds, Neutron Stars: Theory and Observation. Kluwer Academic, Dordrecht, p. 57
Pines D., Alpar M. A., 1985, Nat, 316, 27
Ruderman M., Zhu T., Chen K., 1998, ApJ, 492, 267
Shemar S. L., Lyne A. G., 1996, MNRAS, 282, 677

This paper has been typeset from a TEX/LATEX file prepared by the author.